PHYSICAL REVIEW A **105**, 032804 (2022)

Multiphoton ionization and dissociation of polycyclic aromatic hydrocarbon molecules of astrophysical interest

Roby Chacko,[*] Saroj Barik, Shreyak Banhatti, and G. Aravind[†]
Department of Physics, Indian Institute of Technology Madras, Chennai 600036, India

(Received 4 September 2021; revised 25 November 2021; accepted 17 February 2022; published 10 March 2022)

The photoprocessing of astrophysically relevant small polycyclic aromatic hydrocarbon (PAH) molecules, namely, anthracene, phenanthrene, and pentacene, under intense UV field is experimentally studied to explore the formation of smaller ions upon their dissociative ionization and the effect of their size and structure on the dynamics of dissociative ionization. The molecules are UV processed in the multiphoton regime using a 266-nm nanosecond laser pulse. The dissociative ionization spectra at different laser intensities reveal distinct dissociation dynamics of these PAHs based on their size and structures.

DOI: 10.1103/PhysRevA.105.032804

I. INTRODUCTION

Polycyclic aromatic hydrocarbons (PAHs) are considered to be responsible for the emission in the 3–20-μm range from the interstellar medium (ISM) [1–4], and only a few months back the first PAHs were detected in the ISM [5]. UV photodissociation of PAHs critically determines their ISM abundance [6], particularly with their destructive role overwhelming the slow injection rates of PAHs into the ISM from the circumstellar medium [7]. PAHs are considered as intermediates between small molecules, such as acetylene, and interstellar dust [8], rendering their UV photostability to be of paramount importance. PAHs containing more than 50 carbon atoms are supposed to survive in the interstellar medium while lower sized molecules face photodestruction [9]. Experimental studies on dissociative photoionization of PAH molecules focus on different aspects such as the effects of molecular size [10–12] and structure [13].

Considering the vital role of small hydrocarbons in astrochemistry, we explore their formation via dissociative ionization of PAHs, namely, anthracene, phenanthrene, and pentacene, in the presence of intense UV field. The effects of size and structure of these PAH molecules on the dynamics of dissociative ionization are probed. Previously, we reported our studies on these three PAHs as sources of CH_n^+ ($n = 4$–6) and C_3H_2 in the interstellar medium [13]. A UV laser at 266-nm wavelength is used to probe the dynamics in the photodissociation regions (PDRs), which are impacted by the far-ultraviolet radiation [14].

II. EXPERIMENTAL SETUP

A new experimental setup was built and employed for performing multiphoton ionization (MPI) and multiphoton dissociation (MPD) experiments on PAH molecules. The setup consists of a Wiley-McLaren type of double electric-field time-of-flight mass spectrometer (TOFMS) [15] with a 80-cm-long field-free drift region. The schematic of the setup is shown in Fig. 1.

The repeller electrode is applied at 250 V, and the second and third electrodes are held at 200 V and ground, respectively. The PAH reservoir was heated and diluted with He carrier gas before injecting as supersonic expansion into the interaction region, which is between the repeller and the second electrode of the TOFMS, using a solenoidal pulsed valve. The interaction chamber and the flight tube had a base vacuum of about 10^{-8} mbar. The pulsed valve was operated synchronously with laser shots from the fourth harmonic of a Nd:YAG laser (266 nm) at 10-Hz repetition rate and 4-ns pulse duration. A convex lens of focal length 18.5 cm focused the laser beam to a diameter of 6.3 μm at the interaction region. The experiments were carried out with laser shots of energies 12 to 47 mJ/pulse. This produced laser intensities of the order of 10^{13} W/cm^2, which is sufficient to trigger multiphoton processes. The laser intensities in this paper correspond to a field strength of the order of 1–2 V/Å at the interaction point. The pressure at the interaction region was maintained at not greater than 10^{-5} mbar thus ensuring collisionless character of the molecular photofragmentation processes [16]. The mass resolution ($M/\Delta M$) of the TOFMS was 315. The TOFMS was calibrated by performing MPI of CH_3I (diluted in argon). TOF spectra were obtained with thousands of laser shots.

III. EXPERIMENTAL RESULTS

TOF mass spectra for the multiphoton dissociative ionization of anthracene, phenanthrene, and pentacene are shown in Fig. 2. Anthracene and phenanthrene are isomers ($C_{14}H_{10}$) with 178 amu of mass while pentacene ($C_{22}H_{14}$) has a mass of 278 amu. Anthracene and pentacene are linear chains of aromatic rings while phenanthrene has a kinked structure with a bay region (see insets of TOFMS in Fig. 2). TOFMS for all these three PAHs were collected at various laser intensities. Figure 3 shows higher-mass fragment ions formed from

---

[*] robychako@gmail.com
[†] garavind@iitm.ac.in

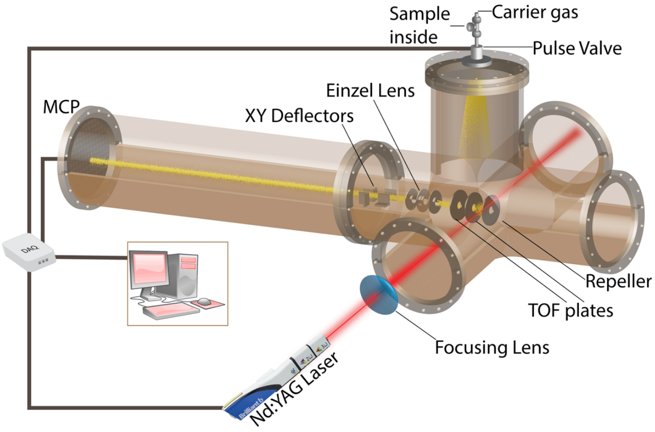

FIG. 1. Schematic of the time-of-flight mass spectrometer setup developed for multiphoton ionization and dissociation experiments.

phenanthrene with increasing laser intensities. Figures 4 and 5 show the variation of ion yield with laser intensity for the prominent higher mass fragments formed from the three molecules.

Spectra of all the three molecules indicate the formation of almost all hydrocarbon groups $C_mH_n^+$, with $m = 1$ to 14, as seen in Fig. 2. Anthracene parent ion yield is meagre when compared to the ionized dissociation products. In contrast with the anthracene, phenanthrene gives a relatively higher yield of the parent ion with hydrogen loss or gain than its ionized fragments. Unlike anthracene and phenanthrene, the parent ion ($C_{22}H_{14}^+$) and any $C_mH_n^+$ cation with $m > 14$ are not observed in the pentacene spectra. Among the hydrocarbon fragment ion groups with mass above 40 amu, $C_{10}H_n^+$ and $C_4H_n^+$ are predominant in all the three spectra.

IV. DISCUSSION

Both computational and experimental works reported on the single-photon absorption spectra of anthracene, phenanthrene, and pentacene reveal a very low cross-section for the resonant absorption at 266 nm [17–25]. Thus, in the present experiment with 266-nm photons we expect the probability of resonant photoabsorption in these three molecules to be extremely weak. The laser intensity varies from 1×10^{13} to 4×10^{13} W/cm^2 as the laser power is changed and this corresponds to field strengths ranging from 0.9 to 1.7 V/Å. The laser intensity values shown in Fig. 3 possess uncertainty of 14 to 16%. The Keldysh parameter determines the ionization process, namely, MPI ($\gamma \gg 1$) and tunnel ionization ($\gamma \ll 1$) [26]. For all the three molecules, at the employed field strengths, the Keldysh adiabaticity parameter (γ) values were estimated to be higher than 1. These values are only indicative as the Keldysh formalism employs zero-range potential which is only an approximation to the real Coulombic potential. In the current experiments, we had reasoned that, apart from the multiphoton processes, field ionization mechanisms (tunnel ionization and barrier suppression ionization) could also contribute to the observed results, as the molecules are relatively larger. (Estimated values of the Keldysh parameter and the reasoning for the presence of field ionization mechanisms in the present experiments are detailed in the Supplemental Material [27].) The ionization potentials of these molecules range from 6 to 8 eV [28–32] and thus the expected order of the MPI process is 2 for all the three molecules. For phenanthrene, which has a strong parent peak in the spectra, the order is measured to be 2.

A. Ionization vs fragmentation

Our results show more extensive fragmentation than intact ionization. Anthracene spectra show a very weak yield for $C_{14}H_n^+$, which includes intact, hydrogenated, and dehydrogenated parent ions. Pentacene spectra are not only void of peaks corresponding to intact parent ions or parent ions with H loss or gain, but also lack any fragments heavier than 200 amu, indicating extensive fragmentation. A startling difference of the spectra of the bent structured phenanthrene compared to the linear species anthracene and the larger molecule pentacene is the high yield of parent ions, despite the nanosecond laser pulse width. The phenanthrene spectra exhibit a small bump at $C_{12}H_n^+$ which includes the acetylene (C_2H_2) loss, whereas the acetylene loss channel is absent in anthracene and pentacene spectra. Phenanthrene differs from anthracene and pentacene in the relative yields for $C_{14}H_n^+$ and $C_{10}H_n^+$ fragments as well.

Various properties of the laser and molecular structure determine the outcomes of the coupling of molecules with intense laser field [33]. In femtosecond photoionization, the pulse length is of the order of molecular vibrations. Thus the degree of nuclear excitation is substantially reduced, leading to the formation of intact parent molecular ions and diminished dissociation. On the other hand, Dewitt *et al.* [34] show that the intact parent ion cannot be detected in the case of ionization of large polyatomic molecular species via nonresonant nanosecond excitation. In an intense radiation field, ionization has to compete with fragmentation, and if the pulse duration is of the order of a picosecond or nanosecond timescale multiple excitations could occur. In multiphoton processes, the molecule has to survive at least two dissociation mechanisms, namely, absorption-dissociation-ionization (ADI) and absorption-ionization-dissociation (AID), to produce parent molecular ions. The ADI mechanism is more probable with nanosecond pulses but weak with femtosecond pulses. High laser fluence could assist in sidestepping ADI and thereby enhancing undissociated parent cation yield [35,36]. AID is more plausible with nanosecond pulses resulting in the decay of parent molecular ions [35]. Though the nonresonant two-photon absorption (a highly anticipated process in the current experiment) is expected to primarily initiate the AID mechanism, in the case of pentacene the ADI mechanism might have dominated since the parent ion is not observed. In short, in the present paper, the nanosecond width of the laser pulses used heavily enhanced AID and ADI mechanisms compared to intact ionization.

Prior works on photoionization and dissociation of PAH molecules show fragmentation to be sensitive to laser intensity [37–39]. These works report parent ion formation, but at three to five orders of lesser intensity than the present paper. Abakumov *et al*. [40] report a prominent parent peak and a peak corresponding to C_2H_2 loss as the main features observed in the multiphoton dissociative ionization, but at a laser

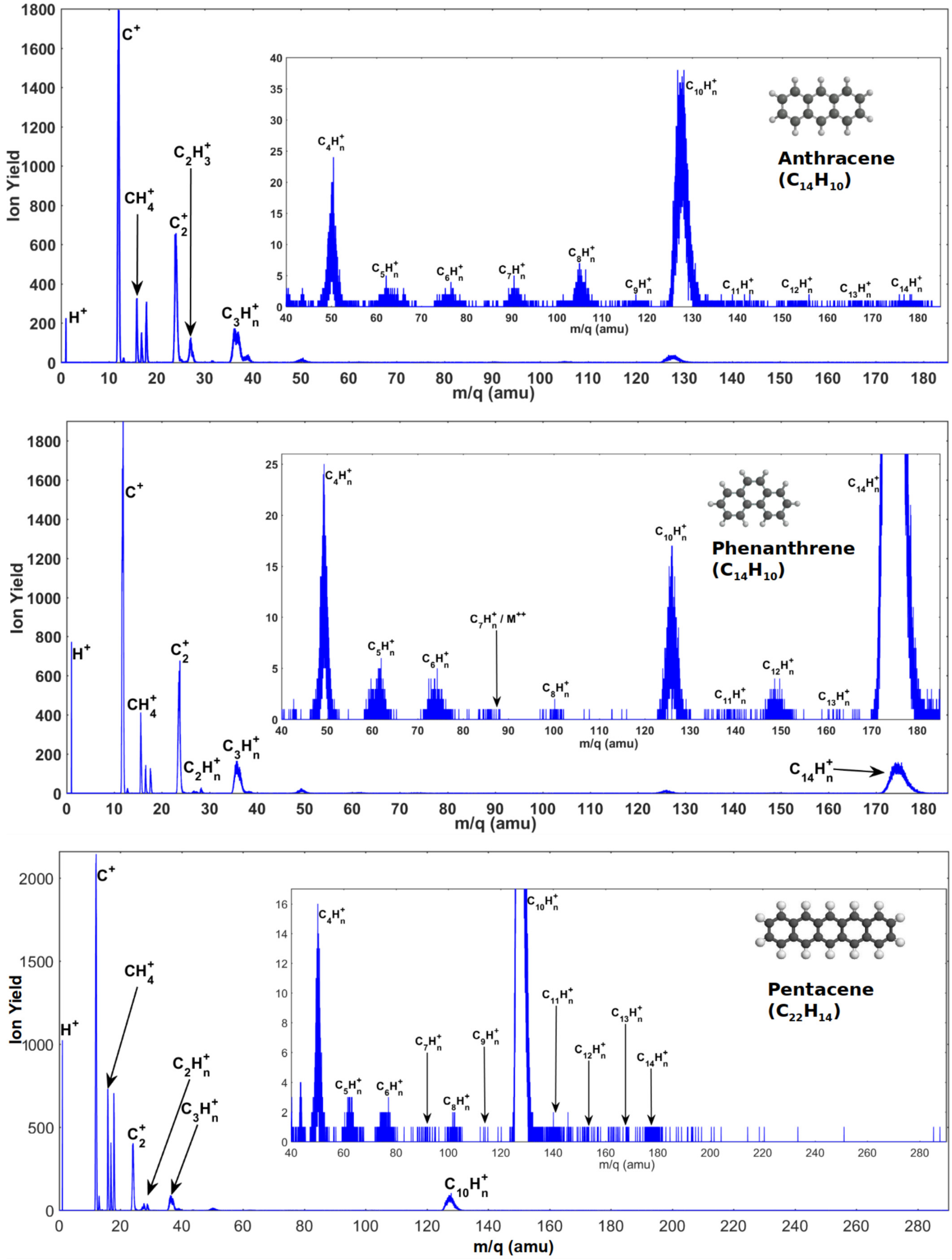

FIG. 2. MPI and MPD spectra of anthracene, phenanthene, and pentacene

intensity of the order of 10^6 W/cm^2 [40]. The pulse width has not been reported in this paper. The present paper as well as the earlier work [41] done with nanosecond pulses at a laser intensity above 10^{10} W/cm^2 do not show this feature. On the other hand, parent ion formation is reported to be prevalent in the femtosecond experiments [36,39,41,42]. These works employ lasers of low photon energy (1.5–1.6 eV) which in turn give better access to different fragmentation channels as the molecules can absorb energies in smaller steps. Unlike in the case of electron impact processes, in photon absorption processes, the whole energy of the photon is dumped into the molecule rather than absorbing the required energy for a transition. Thus, if the photon energy is much higher than the dissociation energy for a particular channel, then this channel

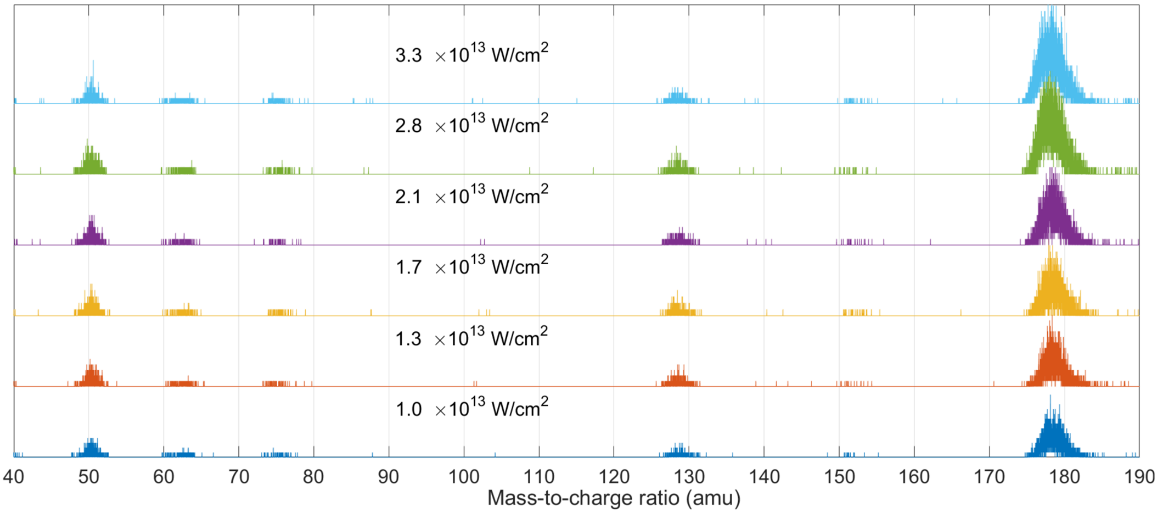

FIG. 3. Phenanthrene MPI and MPD spectra at different laser intensities. Fragments of a mass-to-charge ratio above 40 amu. A vertical offset is maintained to show spectra at different laser intensities separately.

can be omitted as new pathways become accessible with the availability of extra energy. As the PDRs in the interstellar and circumstellar regions are characterized with far-UV photons and a prolonged supply of photons, experiments with UV photons from nanosecond lasers are more relevant than femtosecond IR lasers in the astrophysical context.

The extensive fragmentation observed in the pentacene spectra compared to anthracene and phenanthrene affirms the earlier suggested explanations that fragmentation enhances with an increase in the degrees of freedom, the size of the molecule, density of states, the number of σ-type bonds present in the molecule, and the mean polarizability [43,44]. Coupling of energy from the electronic to the nuclear degrees of freedom is enhanced with increasing density of states and nuclear degrees of freedom. Dewitt *et al.* [34] point out that in a multiphoton coupling mechanism this leads to both molecular fragmentation and an associated reduction in ionization probability. Moreover, the increased density of states in the ionic states of the larger molecules increases the rate of AID, leading to enhanced dissociation. As a result of the enhanced screening due to higher electron number, it is more formidable for the larger molecules to get ionized compared to smaller molecules with fewer delocalized electrons [45]. These effects were observed in many of the earlier reported works [39,43]. Also, pentacene has a higher mean polarizability compared to anthracene and phenanthrene [46], making it more susceptible to external electric fields.

The presence of tunnel ionization (TI) could also be enhancing the fragmentation in the present experiment. Through TI, the neutral parent molecule could transit to the ground cationic state, from which it can access the excited states by absorbing extra photons. This can ease the fragmentation

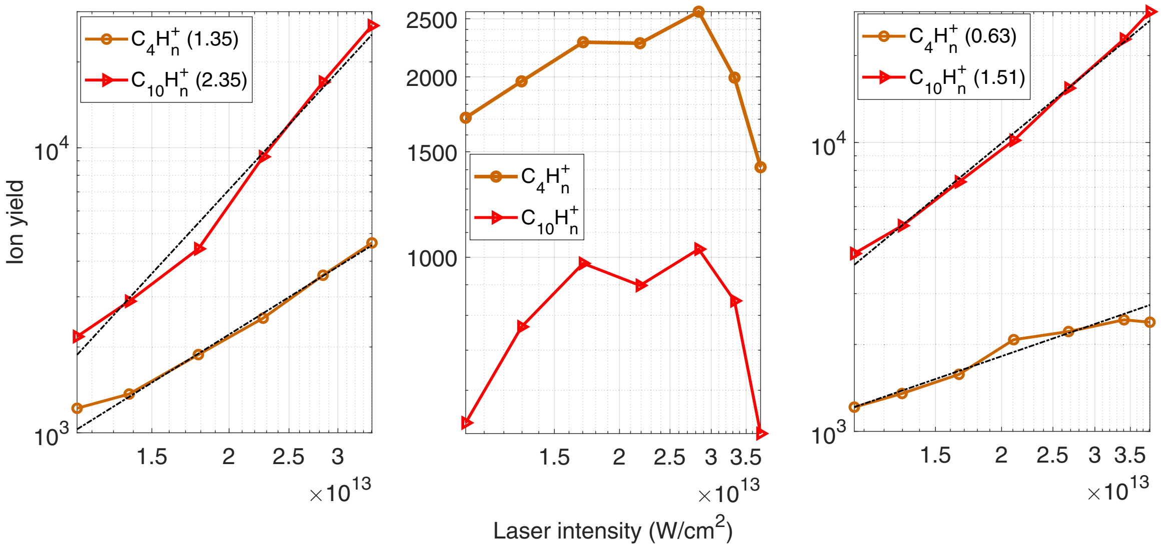

FIG. 4. Laser power dependence of the yield of $C_4H_n^+$ and $C_{10}H_n^+$ from anthracene (left), phenanthrene (middle), and pentacene (right). The numbers in brackets denote the slope of the fitted linear curves for each group.

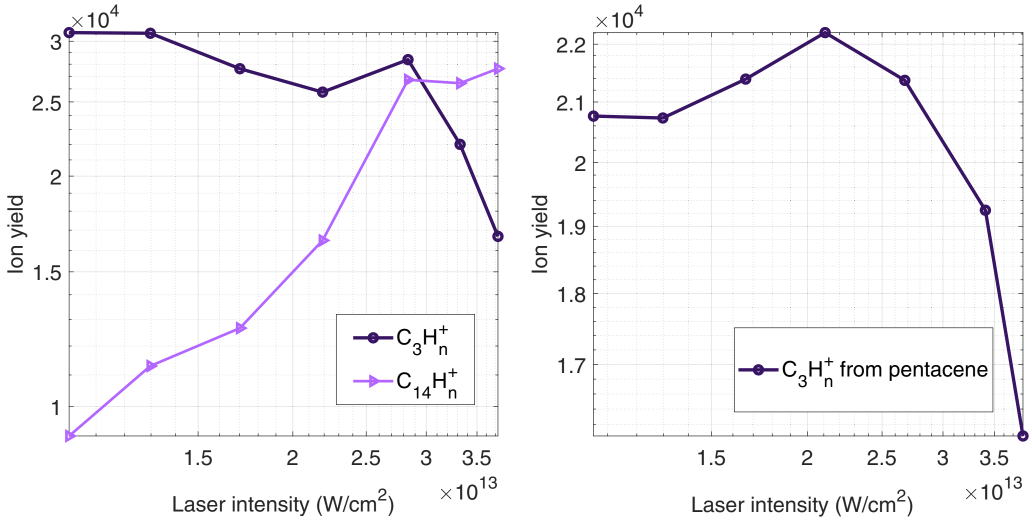

FIG. 5. Left: Laser power dependence of the yield of $C_3H_n^+$ and $C_{14}H_n^+$ fragments from phenanthrene. Right: Laser power dependence of the yield of the $C_3H_n^+$ fragment from pentacene.

processes as it is probable for the cation to end up in some of its dissociative vibrational levels upon photon absorption. The photoelectron spectra (PES) of these molecules [47,48] reveal that there exist many excited states accessible to the ground-state cation within 4.66 eV (single-photon energy). These excited cationic states could themselves be dissociative. The PES reveals that, upon single-photon absorption, the number of accessible cationic states is largest for pentacene (6) when compared to anthracene (4) and phenanthrene (4). Since these cationic states could be dissociative, we can expect more extensive dissociation in pentacene compared to the lower sized anthracene and phenanthrene and we observe the same in our results.

Various factors determine the relative stability of phenanthrene against photofragmentation compared with its isomer anthracene. In comparison with anthracene, phenanthrene is reported to have a higher thermodynamic stability [49], higher delocalization energy or resonance energy [50,51], more Kekule resonance structures, more Clar sextets (leading to greater kinetic stability) [52,53], a lower mean polarizability [46,54], and a topologically more favorable structure for higher stability [55]. A stabilizing hydrogen-hydrogen bond is proposed [56,57] between the H atoms brought closer by the kinked structure in the bay region, based on Bader's "atoms-in-molecules" (AIM) theory [58], but its effect is debated [53,59–61]. According to a density-functional-theory study following the AIM theory by Sabirov [62], the presence of bay regions makes the electronic cloud of the hydrocarbon molecule more compact and less susceptible to external electric fields, resulting in a reduction in the molecular polarizability. Our results on the isomer pairs of anthracene and phenanthrene indicate that the phenanthrene cation has higher survivability against photodissociation compared to anthracene, and this supports the computational work of Sabirov *et al.* [46] which associates minimum polarizability for higher abundance among isomeric interstellar compounds. The heavy fragmentation observed for the more polarizable linear PAH pentacene also corroborates this reasoning.

Another interesting observation from our spectra of anthracene and phenanthrene is the possible presence of the parent dication in the case of phenanthrene. At the same time, there is no indication of a parent dication in the spectra of anthracene. This is notable, as, for the case of dications, the anthracene dication is more stable than the phenanthrene dication [53,63]. Anthracene would have been mainly embracing the ADI mechanism, leaving few parent ions or dications.

B. Yield vs laser intensities

Figure 3 shows the extent of fragmentation at different laser intensities in the case of phenanthrene molecules. (see Supplemental Material [27] for the same in the case of anthracene and pentacene). Figure 2 of the previously reported work [13] shows the same but for fragments with mass less than 40 amu. Figure 4 shows the laser power dependence of fragment ion yield for $C_4H_n^+$ and $C_{10}H_n^+$ formed from anthracene, phenanthrene, and pentacene. The ion yield increases with laser intensity for most fragments from anthracene and pentacene (see Fig. 4 and Fig. 3 of [13]). The fractional values for the slopes, for the linear portion of each curve, implies that in addition to the MPI, field ionization plays a role as well. Presence of multiple channels of formations could also lead to fractional slopes. The general pattern of the laser power dependence of the yield of the ionic fragments formed from phenanthrene differs from anthracene and pentacene as can be seen in Figs. 4 and 5. $C_{14}H_n^+$ tends to get saturated after reaching a threshold. The same feature is reported in [64]. Saturation at higher laser intensities is expected in MPI processes. The heavy fragmentation due to the nanosecond pulse may cause an underestimation of the saturation intensity, I_{sat} [65]. The yield vs laser intensity curves of $C_3H_n^+$, $C_4H_n^+$, and $C_{10}H_n^+$ from phenanthrene and $C_3H_n^+$ from pentacene decline after reaching a maximum. The decline indicates the opening up of new dissociation channels, at a threshold intensity of the laser. The variation of the yield

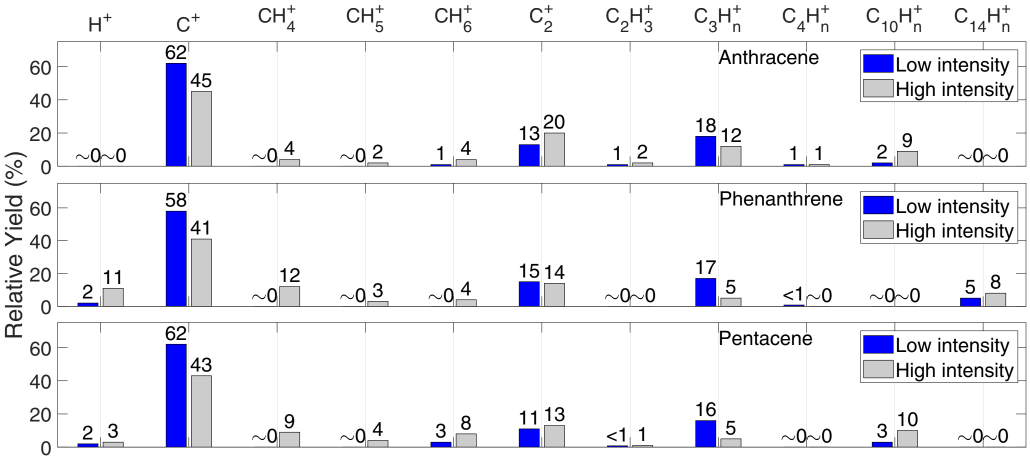

FIG. 6. Relative yield of ionic fragments from anthracene, phenanthrene, and pentacene at lowest laser intensity (blue) and highest laser intensity (gray).

with laser intensities for the lower mass fragments is discussed in the previous work [13].

Figure 6 depicts the percentage yield of the major fragment ions from the anthracene, phenanthrene, and pentacene, respectively, at the lowest and highest laser intensities employed. In all the cases, the major share comes from the C^+ cation the yield of which reduces as the laser intensity increases. This is because of the strengthening up of the other decay channels as well as the opening up of new decay channels. The relative yields of C^+ in the case of all the three molecules at lowest as well as highest laser intensities exhibit striking similarity, irrespective of the difference in the size and structure of the PAH molecules employed. At the lowest laser intensity, $C_3H_n^+$ and C_2^+ hold the second and third places in the relative yield for all the three molecules. Figure 7 shows the variation of the relative yield of C_2^+ and $C_3H_n^+$ with laser intensity for all the three molecules. The complementary feature observed in the case of anthracene is discussed in [13]. In the case of phenanthrene and pentacene, a similar feature is exhibited in the beginning, but as the laser intensity goes high, both C_2^+ and $C_3H_n^+$ start to decline. The complementary yield profile suggests the possibility of the formation of C_2^+ via the decay of $C_3H_n^+$. In the case of phenanthrene and pentacene, the simultaneous decline of C_2^+ and $C_3H_n^+$ at higher laser intensities reveals the opening up of new decay channels for either $C_3H_n^+$ or the preceding species from which $C_3H_n^+$ is formed. Absence of $C_2H_3^+$ is another feature that distinguishes the spectra of phenanthrene from anthracene and pentacene.

Mass spectra of all the three PAH molecules under study show that $C_{10}H_n^+$ and $C_4H_m^+$ are dominant among fragment masses above 40 amu. Among $C_{10}H_n^+$, $C_{10}H_8^+$ (naphthalene cation) is the dominant fragment. $C_4H_2^+$ and $C_4H_3^+$ are the dominant species among $C_4H_m^+$. Previous works indicate that four-carbon hydrocarbon ions occur in stable isomeric forms [66,67]. Separate studies conclude that $C_4H_3^+$ [68,69] and $C_4H_2^+$ [66,70] are resonantly stabilized cations. Dissociation of the parent molecule to neutral $C_{10}H_n$ and C_4H_m species followed by further ionization is a plausible pathway for the formation of $C_{10}H_n^+$ and $C_4H_m^+$ ions. $C_{10}H_n^+$ can also form from $C_{14}H_{10}^+$ via C_4H_m loss. The neutral C_4H_m can further undergo photoionization, giving $C_4H_m^+$. The striking similarity

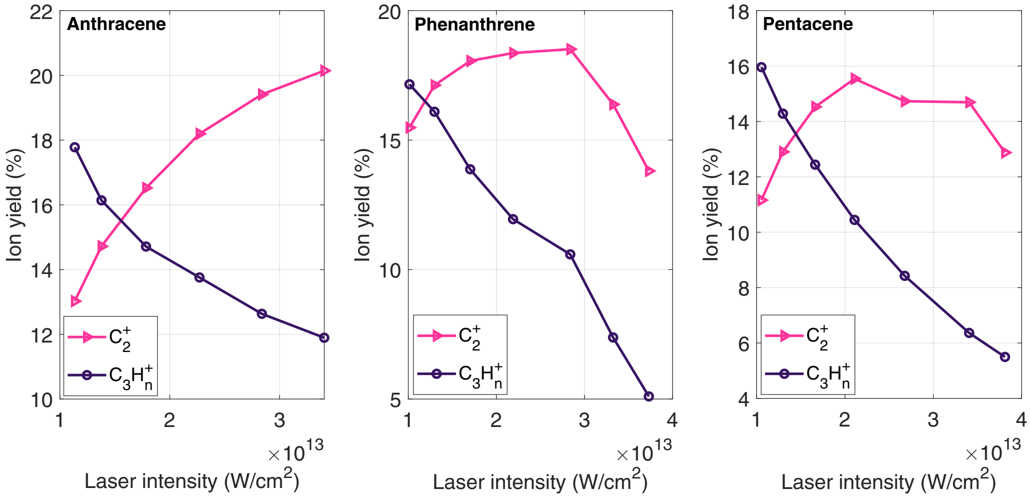

FIG. 7. Variation of the relative yield of the ionic fragments C_2^+ and $C_3H_n^+$ with different laser intensities

in the variation of the ion yield with laser intensities of $C_{10}H_n^+$ and $C_4H_m^+$ from the phenanthrene parent (see Fig. 4) suggests a similarity at the beginning of their formation pathways. A noticeable difference in the formation of $C_{10}H_n^+$ from phenanthrene compared to anthracene and pentacene is the very low share in the total ion yield. The share is less than 0.5% for $C_{10}H_n^+$ from phenanthrene, whereas $C_{10}H_n^+$ from anthracene and pentacene exhibits a maximum of 9 to 10% share (see Fig. 6).

V. SUMMARY

The multiphoton ionization and dissociation of small PAH molecules of astrophysical interest, namely, anthracene, phenanthrene, and pentacene, under intense UV field generated by a nanosecond laser pulse are studied using a newly constructed experimental setup. The experiments are performed at different laser intensities and the results provide a wealth of information regarding the fragmentation patterns. The effects of the size and structure of PAH molecules upon coupling with intense UV field are specially studied. The phenanthrene molecule, with a bent structure, exhibits a variety of different features compared to the linear benzenoids anthracene and pentacene. Phenanthrene is found to be more photostable than anthracene and pentacene in the UV regions of the interstellar and circumstellar environments. The present results shed light on the structure and dynamics of the PAH components of the interstellar medium and are of paramount importance for astrophysical models explaining interstellar chemistry.

ACKNOWLEDGMENTS

This work was supported by the Board of Research in Nuclear Sciences under Project No. 2012/37P/45/BRNS.

---

[1] E. Peeters, Proc. International Astronomical Union **7**, 149 (2011).

[2] F. Salama, G. A. Galazutdinov, J. Krełowski, L. J. Allamandola, and F. A. Musaev, Astrophys. J. **526**, 265 (1999)

[3] F. Salama, E. L. O. Bakes, L. J. Allamandola, and A. G. G. M. Tielens, Astrophys. J. **458**, 621 (1996).

[4] L. J. Allamandola, A. G. G. M. Tielens, and J. R. Barker, in *Physical Processes in Interstellar Clouds*, edited by G. E. Morfill and M. Scholer, NATO ASI Series C: Mathematical and Physical Sciences Vol. 210 (Springer, New York, 1987), pp. 305–331.

[5] B. A. McGuire, R. A. Loomis, A. M. Burkhardt, K. L. K. Lee, C. N. Shingledecker, S. B. Charnley, I. R. Cooke, M. A. Cordiner, E. Herbst, S. Kalenskii *et al.*, Science **371**, 1265 (2021).

[6] T. P. Snow, V. Le Page, Y. Keheyan, and V. M. Bierbaum, Nature (London) **391**, 259 (1998).

[7] H. W. Jochims, E. Ruhl, H. Baumgartel, S. Tobita, and S. Leach, Astrophys. J. **420**, 307 (1994).

[8] J. L. Puget and A. Léger, Annu. Rev. Astron. Astrophys. **27**, 161 (1989).

[9] T. Allain, S. Leach, and E. Sedlmayr, Astron. Astrophys. **305**, 602 (1996).

[10] G. Wenzel, C. Joblin, A. Giuliani, S. Rodriguez Castillo, G. Mulas, M. Ji, H. Sabbah, S. Quiroga, D. Peña, and L. Nahon, Astron. Astrophys. **641**, A98 (2020).

[11] J. Zhen, P. Castellanos, D. M. Paardekooper, N. Ligterink, H. Linnartz, L. Nahon, C. Joblin, and A. G. G. M. Tielens, Astrophys. J. **804**, L7 (2015).

[12] J. Zhen, S. R. Castillo, C. Joblin, G. Mulas, H. Sabbah, A. Giuliani, L. Nahon, S. Martin, J.-P. Champeaux, and P. M. Mayer, Astrophys. J. **822**, 113 (2016).

[13] R. Chacko, S. Banhatti, S. Barik, and G. Aravind, Astrophys. J. **896**, 130 (2020).

[14] D. J. Hollenbach and A. G. G. M. Tielens, Annu. Rev. Astron. Astrophys. **35**, 179 (1997).

[15] W. C. Wiley and I. H. McLaren, Rev. Sci. Instrum. **26**, 1150 (1955).

[16] V. S. Antonov and V. S. Letokhov, Appl. Phys. **24**, 89 (1981).

[17] T. M. Halasinski, D. M. Hudgins, F. Salama, L. J. Allamandola, and T. Bally, J. Phys. Chem. A **104**, 7484 (2000).

[18] T. Kitagawa, J. Mol. Spectrosc. **26**, 1 (1968).

[19] A. Thöny and M. J. Rossi, J. Photochem. Photobiol. A: Chemistry **104**, 25 (1997).

[20] J. Ferguson, L. W. Reeves, and W. G. Schneider, Can. J. Chem. **35**, 1117 (1957).

[21] R. Dygdała and K. Stefański, Chem. Phys. **53**, 51 (1980).

[22] K. H. Hardtl and A. Scharmann, Z. Naturforsch. **12**, 715 (1957).

[23] P. Sony and A. Shukla, Phys. Rev. B **75**, 155208 (2007).

[24] G. Malloci, G. Mulas, and C. Joblin, Astron. Astrophys. **426**, 105 (2004).

[25] I. Benkyi, E. Tapavicza, H. Fliegl, and D. Sundholm, Phys. Chem. Chem. Phys. **21**, 21094 (2019).

[26] L. V. Keldysh, ZhETF **47**, 1945 (1965) [Sov. Phys. JETP **20**, 1307 (1965)].

[27] See Supplemental Material at http://link.aps.org/supplemental/10.1103/PhysRevA.105.032804 for a detailed discussion on the estimated values of keldysh parameters, and description about some unique features observed in the MPI and MPD spectra of phenanthrene.

[28] G. Briegleb, Angew. Chem., Int. Ed. Engl. **3**, 617 (1964).

[29] P. A. Clark, F. Brogli, and E. Heilbronner, Helv. Chim. Acta **55**, 1415 (1972).

[30] M. Meot-Ner, J. Phys. Chem. **84**, 2716 (1980).

[31] D. Stahl and F. Maquin, Chem. Phys. Lett. **108**, 613 (1984).

[32] J. W. Hager and S. C. Wallace, Anal. Chem. **60**, 5 (1988).

[33] A. Konar, Y. Shu, V. V. Lozovoy, J. E. Jackson, B. G. Levine, and M. Dantus, J. Phys. Chem. A **118**, 11433 (2014).

[34] M. J. Dewitt and R. J. Levis, J. Chem. Phys. **110**, 11368 (1999).

[35] R. J. Levis and M. J. DeWitt, J. Phys. Chem. A **103**, 6493 (1999).

[36] M. Murakami, M. Tanaka, T. Yatsuhashi, and N. Nakashima, J. Chem. Phys. **126**, 104304 (2007).

[37] J. Poveda, A. Guerrero, I. Álvarez, and C. Cisneros, J. Photochem. Photobiol. A: Chemistry **215**, 140 (2010).

[38] J. Poveda, I. Álvarez, and C. Cisneros, J. Photochem. Photobiol. A: Chemistry **230**, 31 (2012).

[39] L. Robson, A. Tasker, K. Ledingham, P. McKenna, T. McCanny, C. Kosmidis, P. Tzallas, D. Jaroszynski, and D. Jones, Int. J. Mass Spectrom. **220**, 69 (2002).
[40] G. A. Abakumov, Y. M. Anisimov, S. E. Kupriyanov, R. V. Manvelyan, A. A. Petrov, and A. P. Simonov, Sov. J. Quantum Electron. **11**, 268 (1981).
[41] M. J. DeWitt and R. J. Levis, J. Chem. Phys. **102**, 8670 (1995).
[42] A. N. Markevitch, D. A. Romanov, S. M. Smith, and R. J. Levis, Phys. Rev. A **75**, 053402 (2007).
[43] A. N. Markevitch, N. P. Moore, and R. J. Levis, Chem. Phys. **267**, 131 (2001).
[44] A. N. Markevitch, D. A. Romanov, S. M. Smith, H. B. Schlegel, M. Y. Ivanov, and R. J. Levis, Phys. Rev. A **69**, 013401 (2004).
[45] M. Kjellberg, A. V. Bulgakov, M. Goto, O. Johansson, and K. Hansen, J. Chem. Phys. **133**, 074308 (2010).
[46] D. S. Sabirov, R. R. Garipova, and F. Cataldo, Molecular Astrophys. **12**, 10 (2018).
[47] R. Boschi, J. N. Murrell, and W. Schmidt, Faraday Discuss. Chem. Soc. **54**, 116 (1972).
[48] R. Boschi, E. Clar, and W. Schmidt, J. Chem. Phys. **60**, 4406 (1974).
[49] I. Gutman and S. Stanković, Macedonian J. Chem. Chem. Eng. **26**(2), 111 (2007).
[50] L. Pauling, *The Nature of the Chemical Bond and the Structure of Molecules and Crystals: An Introduction to Modern Structural Chemistry*, 3rd ed. (Cornell University, Ithaca, 1960).
[51] R. Kalescky, E. Kraka, and D. Cremer, J. Phys. Chem. A **118**, 223 (2014).
[52] M. Solà, Front. Chem. **1**, 4 (2013).
[53] J. Poater, M. Duran, and M. Solà, Front. Chem. **6** (2018).
[54] A. Hinchliffe and H. Soscun Machado, Int. J. Molecular Sci. **1**, 8 (2000).
[55] A. Ciesielski, T. M. Krygowski, and M. K. Cyrański, J. Chem. Info. Modeling **48**, 1358 (2008).
[56] C. F. Matta, J. Hernández-Trujillo, T.-H. Tang, and R. F. W. Bader, Chem. A: European J. **9**, 1940 (2003).
[57] A. V. Vashchenko and T. N. Borodina, J. Struct. Chem. **54**, 479 (2013).
[58] R. F. W. Bader, *Atoms in Molecules: A Quantum Theory*, International Series of Monographs on Chemistry (Oxford University, London, 1990).
[59] J. Poater, R. Visser, M. Solà, and F. M. Bickelhaupt, J. Organic Chem. **72**, 1134 (2007).
[60] S. Grimme, C. Mück-Lichtenfeld, G. Erker, G. Kehr, H. Wang, H. Beckers, and H. Willner, Angew. Chem., Int. Ed. **48**, 2592 (2009).
[61] R. D. Hancock and I. V. Nikolayenko, J. Phys. Chem. A **116**, 8572 (2012).
[62] D. Sabirov, Comput. Theore. Chem. **1030**, 81 (2014).
[63] J. Dominikowska and M. Palusiak, Phys. Chem. Chem. Phys. **13**, 11976 (2011).
[64] C. Gehm, T. Streibel, J. Passig, and R. Zimmermann, Applied Sciences **8**, 1617 (2018).
[65] R. Mizoguchi, Y. Shimada, H. Shinohara, T. Yatsuhashi, and N. Nakashima, Rev. Laser Eng. **32**, 717 (2004).
[66] P. P. Bera, R. Peverati, M. Head-Gordon, and T. J. Lee, Phys. Chem. Chem. Phys. **17**, 1859 (2015).
[67] G. Angelova, O. Novotny, J. Mitchell, C. Rebrion-Rowe, J. Le Garrec, H. Bluhme, K. Seiersen, and L. Andersen, Int. J. Mass Spectrom. **232**, 195 (2004).
[68] R. I. Kaiser, A. Mebel, O. Kostko, and M. Ahmed, Chem. Phys. Lett. **485**, 281 (2010).
[69] N. Hansen, S. J. Klippenstein, C. A. Taatjes, J. A. Miller, J. Wang, T. A. Cool, B. Yang, R. Yang, L. Wei, C. Huang *et al.*, J. Phys. Chem. A **110**, 3670 (2006).
[70] Y. Zhao, S.-q. Wan, H.-l. Liu, X.-r. Huang, and C.-c. Sun, Chem. Res. Chin. Universities **29**, 150 (2013).